European Journal of Neuroscience, Vol. 20, pp. 3322–3330, 2004

Presynaptic localization of an AMPA-type glutamate receptor in corticostriatal and thalamostriatal axon terminals

Fumino Fujiyama,[1] Eriko Kuramoto,[1] Keiko Okamoto,[1] Hiroyuki Hioki,[1] Takahiro Furuta,[1] Ligang Zhou,[1] Sakashi Nomura[2] and Takeshi Kaneko[1,3]
[1]Department of Morphological Brain Science, Graduate School of Medicine, Kyoto University, Japan
[2]Department of Physical Therapy, School of Health Sciences, Faculty of Medicine, Kyoto University, Japan
[3]CREST, JST, Kyoto 606–8501, Japan

Keywords: autoreceptor, immuno-electron microscopy, neostriatum, rat, vesicular glutamate transporter

Abstract

The neostriatum is known to receive glutamatergic projections from the cerebral cortex and thalamic nuclei. Vesicular glutamate transporters 1 and 2 (VGluT1 and VGluT2) are located on axon terminals of corticostriatal and thalamostriatal afferents, respectively, whereas VGluT3 is found in axon terminals of cholinergic interneurons in the neostriatum. In the present study, the postsynaptic localization of ionotropic glutamate receptors was examined in rat neostriatum by the postembedding immunogold method for double labelling of VGluT and glutamate receptors. Immunoreactive gold particles for AMPA receptor subunits GluR1 and GluR2/3 were frequently found not only on postsynaptic but also on presynaptic profiles immunopositive for VGluT1 and VGluT2 in the neostriatum, and GluR4-immunoreactive particles were observed on postsynaptic and presynaptic profiles positive for VGluT1. Quantitative analysis revealed that 27–45% of GluR1-, GluR2-, GluR2/3- and GluR4-immunopositive particles found in VGluT1- or VGluT2-positive synaptic structures in the neostriatum were associated with the presynaptic profiles of VGluT-positive axons. In contrast, VGluT-positive presynaptic profiles in the neostriatum showed almost no immunoreactivity for NMDA receptor subunits NR1 or NR2A/B. Furthermore, almost no GluR2/3-immunopositive particles were observed in presynaptic profiles of VGluT3-positive (cholinergic) terminals that made asymmetric synapses in the neostriatum, or in those of VGluT1- or VGluT2-positive terminals in the neocortex. The present results indicate that AMPA receptor subunits but not NMDA receptor subunits are located on axon terminals of corticostriatal and thalamostriatal afferents, and suggest that glutamate released from these axon terminals controls the activity of the terminals through the presynaptic AMPA autoreceptors.

Introduction

The neostriatum receives glutamatergic excitatory afferents mostly from the cerebral cortex and intralaminar thalamic nuclei (for review, see Smith & Bolam, 1990). Synaptic transmission of these corticostriatal and thalamostriatal pathways are considered to play a crucial role in motor control, cognitive functions and plasticity (for review, see Calabresi *et al*., 2000) and in neurodegenerative disorders of the basal ganglia, such as Parkinson's and Huntington's diseases (for review, see Alexi *et al*., 2000). The multiple actions of glutamate are mediated by an array of receptors that are divided into two distinct groups, ionotropic and metabotropic receptors (for review, see Ozawa *et al*., 1998). The ionotropic receptors are further divided pharmacologically into NMDA, kainate and AMPA subtypes. In particular, AMPA receptors mediate fast excitatory neurotransmission in most excitatory synapses of the central nervous system including the neostriatum. Furthermore, AMPA receptors have been characterized on a molecular basis and revealed to be composed of homomeric or heterometic oligomers of subunits, GluR1 to GluR4 (for review, see Ozawa *et al*., 1998).

Correspondence: Dr Takeshi Kaneko, [1]Department of Morphological Brain Science, as above.
E-mail: kaneko@mbs.med.kyoto-u.ac.jp

Received 4 February 2004, revised 1 October 2004, accepted 12 October 2004

doi:10.1111/j.1460-9568.2004.03807.x

Although AMPA receptors are located at the postsynaptic membrane to produce excitatory postsynaptic potentials in most brain regions, microdialysis experiments (Patel *et al*., 2001) have recently suggested that glutamate works on presynaptic AMPA-type autoreceptors of glutamatergic axon terminals in the neostriatum. Because the presynaptic localization of AMPA receptor subunits have so far only occasionally been observed in the neostriatum by immunoperoxidase electron microscopy (though data not shown in Bernard *et al*., 1997), the presynaptic localization should be studied more precisely by electron microscopy with higher subcellular resolution such as the immunogold method. Furthermore, the possibility of AMPA-type autoreceptors on the glutamatergic terminals raises another question: what kind of glutamatergic afferents to the neostriatum have presynaptic AMPA receptors?

The two major excitatory afferents to the neostriatum, corticostriatal and thalamostriatal afferents, can be differentiated by the expression of vesicular glutamate transporters (VGluTs). Messenger RNA for VGluT1 but not for VGluT2 is expressed massively in neocortical neurons including layer V corticostriatal neurons, whereas VGluT2 mRNA but not VGluT1 mRNA is highly enriched in the thalamic nuclei (Ni *et al*., 1994, 1995; Hisano *et al*., 2000; Bai *et al*., 2001; Fremeau *et al*., 2001; Herzog *et al*., 2001). Thus, corticostriatal and thalamostriatal axon terminals can be separately labelled with antibodies to VGluT1 and VGluT2, respectively. In addition, the

neostriatum contains the third type of putatively glutamatergic axon terminal, which is derived from cholinergic striatal interneurons and loaded with VGluT3 (Gras *et al*., 2002). In the present study, we examined the electron-microscopic localization of AMPA receptor subunits at presynaptic profiles of those three kinds of glutamatergic axon terminals in rat neostriatum by using the postembedding immunogold method for double labelling of VGluT and glutamate receptors.

Materials and methods

The experiments were conducted according to the rules of animal care and use of Graduate School of Medicine, Kyoto University. In the experiments, we used adult male Wistar rats (200–300 g body weight; Japan SLC, Shizuoka, Japan), and tried to minimize the number of animals.

Confocal laser scanning microscopic analysis

Three rats were deeply anaesthetized by intraperitoneal injection of chloral hydrate (350 mg/kg body weight). Ten percent biotinylated dextran amine (BDA; Molecular Probes, Eugene, OR, USA) dissolved in phosphate-buffered saline (PBS) was stereotaxically injected into the intralaminar thalamic nuclei or sensorimotor cortex by passing positive current pulses (2 μA, 7 s, 1/14 Hz) for 12 min through a glass micropipette, and the rats were allowed to survive for 7–10 days. The injected rats and two normal rats were deeply anaesthetized (700 mg chloral hydrate/kg) and perfused with 200 mL of PBS, followed by 300 mL of 0.2% formaldehyde, 0.02% glutaraldehyde, 75% saturated picric acid and 0.1 M Na_2HPO_4, pH 7.4 (adjusted with NaOH), followed by immersion for 4 h at 4 °C in 2% formaldehyde, 75% saturated picric acid and 0.1 M Na_2HPO_4, pH 7.4. After fixation and cryoprotection, brain blocks through the neostriatum were cut into 30-μm-thick frontal sections on a freezing microtome.

The sections from the BDA-injected rats were incubated overnight with 1 μg/mL affinity-purified rabbit antibody to VGluT1, VGluT2 or VGluT3 (Hioki *et al*., 2003, 2004), and then for 1 h with a mixture of 1 μg/mL fluorescein-conjugated avidin D (Vector, Burlingame, CA, USA) and 10 μg/mL Alexa546-labelled antirabbit IgG goat antibody (Molecular Probes). All the incubations were carried out at room temperature in PBS containing 0.25% λ-carrageenan, 0.5% normal donkey serum, 0.3% Triton X-100 and 0.02% sodium azide, and followed by a rinse with PBS containing 0.3% Triton X-100.

The sections from the normal rats were stained for double immunofluorescence as described before (Fujiyama *et al*., 2001), using guinea pig antibodies to VGluT1-3 (1 μg/mL; Fujiyama *et al*., 2001; Hioki *et al*., 2004), rabbit antibodies to VGluT1-3 (1 μg/mL; Hioki *et al*., 2003, 2004) and tyrosine hydroxylase (1 : 2000 dilution; Chemicon, Temecula, CA, USA), and goat antibody to vesicular acetylcholine transporter (1 : 2000; Chemicon). Briefly, the sections were incubated overnight with a mixture of a guinea pig primary antibody and either a rabbit or goat primary antibody, and then for 1 h with biotinylated anti-guinea pig IgG donkey antibody (10 μg/mL; Chemicon). Finally, the sections were incubated for 1 h with a mixture of 1 μg/mL Alexa647-conjugated streptoavidin (Molecular Probes) and 10 μg/mL Alexa488-conjugated goat or donkey antibody to rabbit or goat IgG (Molecular Probes).

The stained sections were mounted on glass slides, air dried and coverslipped with 50% glycerol and 2.5% triethylenediamine in PBS. Fluorescence was observed under a confocal laser scanning microscope LSM5 Pascal (Zeiss, Oberkochen, Germany). When one of the primary antibodies was omitted or replaced with normal IgG, no immunofluorescence for the omitted or replaced antibody was detected.

Double immunoelectron-microscopic labelling after embedding

Nine rats were deeply anaesthetized (700 mg chloral hydrate/kg) and perfused transcardially with 200 mL of PBS, followed by 300 mL of 4% paraformaldehyde and 0.1% glutaraldehyde in 0.1 M phosphate–NaOH buffer, pH 7.4 (PB). The removed brains were postfixed at 4 °C for 3 h with 4% paraformaldehyde and 0.1% glutaraldehyde in PB. The neostriatal blocks were cut into 500-μm-thick frontal sections on a vibratome. The sections were freeze-substituted and embedded in resin according to Nusser *et al*. (1998). Briefly, after a wash with PB the sections were cryoprotected by incubation for 1 h with 0.5 M sucrose and then for 2 h with 1 M sucrose in PB. They were slammed on a copper plate (MM80E; Leica, Vienna, Austria) cooled with liquid nitrogen. The frozen sections were embedded in resin Lowicryl HM20 (Polysciences, Inc., Eppelheim, Germany) by automatic freeze substitution system EM AFS (Leica) with the following protocol: the sections were (i) placed for 36 h at −80 °C in methanol, followed by a gradual increase of temperature for 3 h to −50 °C; (ii) sequentially immersed for 1.5 h each at −50 °C in a 1 : 1 mixture and then a 1 : 2 mixture of methanol and resin and then twice in resin alone, followed by incubation overnight at −50 °C in resin; and (iii) after a change of resin, polymerized under ultraviolet light for 48 h at −50 °C for 7 h with a gradual temperature increase to +20 °C and finally for 24 h at +20 °C. After polymerization, the sections were cut into 70-nm-thick ultrathin sections on an ultramicrotome (Reichert-Nissei Ultracut S, Leica).

The ultrathin sections were collected on grids and doubly immunolabelled for VGluT and glutamate receptors. After etching with 10% H_2O_2, the sections on the grids were blocked for 30 min with 2% human serum albumin in 50 mM Tris–HCl-buffered 0.9% saline, pH 7.4 (TBS), followed by solubilization for 30 min with TBS containing 0.01% Triton X-100 (TBS-T). The sections were then incubated overnight at 4 °C in TBS-T containing 2% human serum albumin (TBS-TA) with a mixture of affinity-purified guinea pig antibody against VGluT1, VGluT2 or VGluT3 (1 μg/mL) and one of the following rabbit or mouse antibodies (1 μg/mL, unless otherwise described): rabbit antibodies against rat GluR1 C-terminal (Chemicon; Upstate, New York, NY, USA), rat GluR2/3 C-terminal (Chemicon; Upstate), rat GluR4 C-terminal (Chemicon; Upstate), rat NR1 C-terminal (Chemicon) and rat NR2A/B C-terminal (Chemicon); and mouse IgGs against GluR2[175–430] (MAB397; Chemicon) and rat GluR3[245–451] (MAB5416; Chemicon). The antibodies against GluR1–4 recognized common sites for their flip and flop alternative forms.

After a wash with TBS, the sections were further incubated for 2 h in TBS-TA with a mixture of 1 : 20-diluted anti-guinea pig IgG goat antibody coupled with 10-nm gold particles (BioCell; Cardiff, UK) and 1 : 20-diluted anti-rabbit IgG or anti-mouse IgG goat antibody conjugated with 15-nm gold particles (Amersham, Bucks, UK). After labelling, the sections were washed with TBS, stained with 1% uranyl acetate and examined with electron microscope H-7100 (Hitachi, Tokyo, Japan). When one of the primary antibodies was omitted or replaced with normal IgG, immunogold labelling for the omitted or replaced antibody was considered to represent the background level, which was usually very low. As a control for GluR2/3 C-terminal, the antibody was pre-incubated with an excess amount (1 : 10 000 molar ratio) of antigen peptide EGYNVYGIESVKI. After a mixture of

antibodies to GluR2/3 and VGluT was pre-incubated for 1 h with the antigen peptide, the ultrathin sections were immunolabelled with the mixture as described above. For sampling of each combination of VGluT and GluR in the postembedding electron microscopic method, at least three different rats were examined and taken into the data for quantitative analysis.

For the pre-embedding immunoelectron microscopy, three rats were used. VGluT immunoreactivity was labelled by the immunogold and silver enhancement method as described in the previous studies (Fujiyama *et al*., 2001; Kaneko *et al*., 2002). All the black and white electron-microscopic photographs were printed and digitized with a scanner at a 300-dpi resolution. These digital images and those from the confocal laser-scanning microscopic study were arranged using Canvas (Deneba Systems, Miami, FL, USA) with some contrast enhancement (10–30%), and saved as TIFF files.

Results

Sources of VGluT-immunoreactive terminals

Under the confocal laser-scanning microscope, BDA-labelled corticostriatal and thalamostriatal axon terminals were reacted for VGluT1 and VGluT2, respectively (Fig. 1a–d). No colocalization between VGluT1 and VGluT2 immunoreactivities was found in single axon terminal-like profiles of the neostriatum (Fig. 1e). These results together with previous *in situ* hybridization studies (Ni *et al*., 1994, 1995; Hisano *et al*., 2000; Bai *et al*., 2001; Fremeau *et al*., 2001; Herzog *et al*., 2001) indicate that the corticostriatal and thalamostriatal afferents use VGluT1 and VGluT2, respectively, for the uptake of glutamate into synaptic vesicles. Because VGluT2 mRNA might be distributed in the mesencephalic ventral tegmental region including the substantia nigra (Fremeau *et al*., 2001), we examined the colocalization of tyrosine hydroxylase and VGluT2 in the neostriatum but did not find any colocalization in single axon terminals.

VGluT3-immunoreactive axon terminals were negative for VGluT1 or VGluT2 (Fig. 1f and g), but positive for vesicular acetylcholine transporter (Fig. 1h). This result suggests that the VGluT3-immunoreactive axon terminals originated from cholinergic interneurons and that these interneurons may use both glutamate and acetylcholine as their neurotransmitter. Thus, VGluT1, VGluT2 and VGluT3 immunoreactivities are considered to be markers for corticostriatal, thalamostriatal and intrinsic glutamatergic axon terminals, respectively, in the neostriatum.

Glutamate receptors in asymmetric synapses that are formed with VGluT-immunopositive axon terminals

We then examined the localization of ionotropic glutamate receptors in synapses formed with VGluT-immunoreactive axon terminals. By the pre-embedding immunogold–silver enhancement method, VGluT-immunoreactive silver grains were associated mostly with synaptic vesicles and much less frequently with presynaptic membranes of asymmetric synapses in the neostriatum (Fig. 1i and j). Because it is well known that ionotropic glutamate receptors in synaptic sites are difficult to label by the pre-embedding immunostaining method (Chatha *et al*., 2000), we examined glutamate receptor immunoreactivities in VGluT-positive synapses by the postembedding immunogold technique with freeze-substitution. Presynaptic profiles with 10-nm immunogold particles for VGluT1, VGluT2 and VGluT3 invariably formed asymmetric synapses in the neostriatum (Figs 2 and 3). Inversely, VGluT1-, VGluT2- and VGluT3-immunoreactive gold particles were found in ≈40, 30 and < 10%, respectively, of the axon terminals making asymmetric synapses in the neostriatum, indicating good labelling efficiency for VGluT in the present immunogold method. By contrast, although the rabbit antibodies to rat GluR2/3 C-terminal and GluR1 C-terminal resulted in the best labelling of the

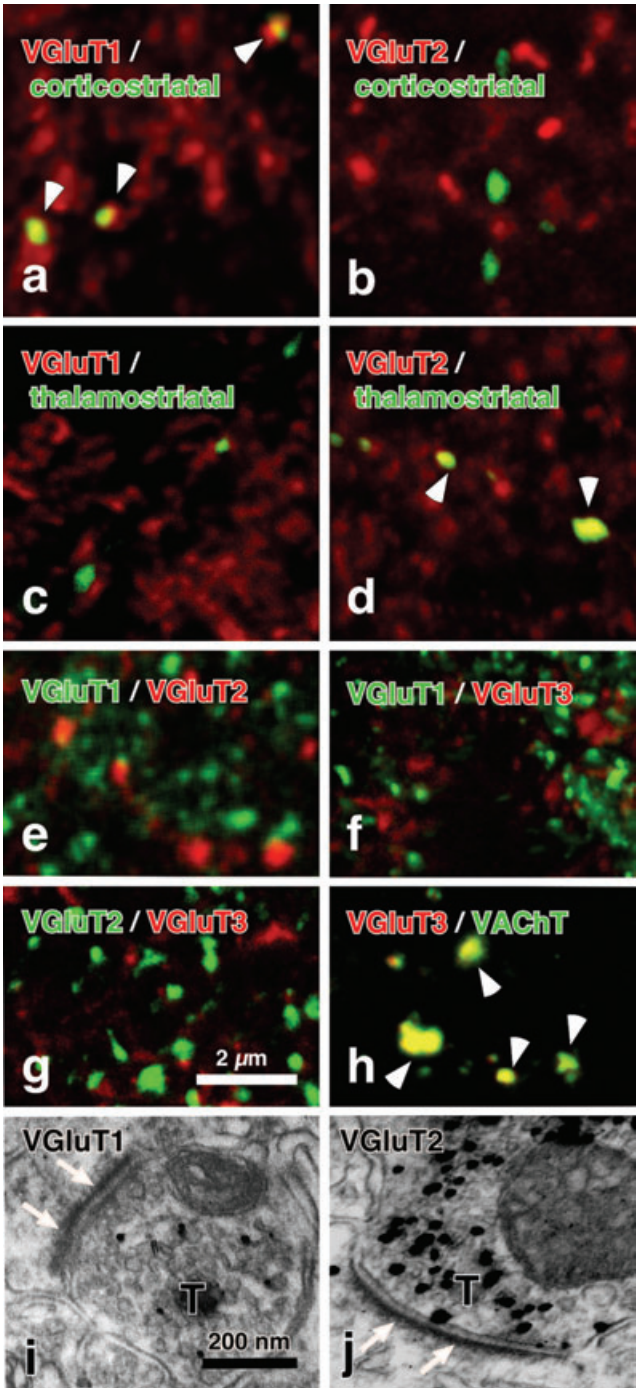

FIG. 1. Axon terminal-like profiles with VGluT immunoreactivity in the neostriatum. (a–d) BDA-labelled afferent terminals are visualized with fluorescein-conjugated avidin. Arrowheads indicate yellow profiles showing colocalization of green fluorescence (fluorescein in a–d; Alexa488 in e–h) and red or dark red fluorescence (Alexa546 in a–d; Alexa647 in e–h). Arrows in electron-micrographs i and j point to the postsynaptic specialization. For further detail, see Results. VAChT, vesicular acetylcholine transporter; T, axon terminal. Scale bar in g applies to a–h; that in i applies to i and j.

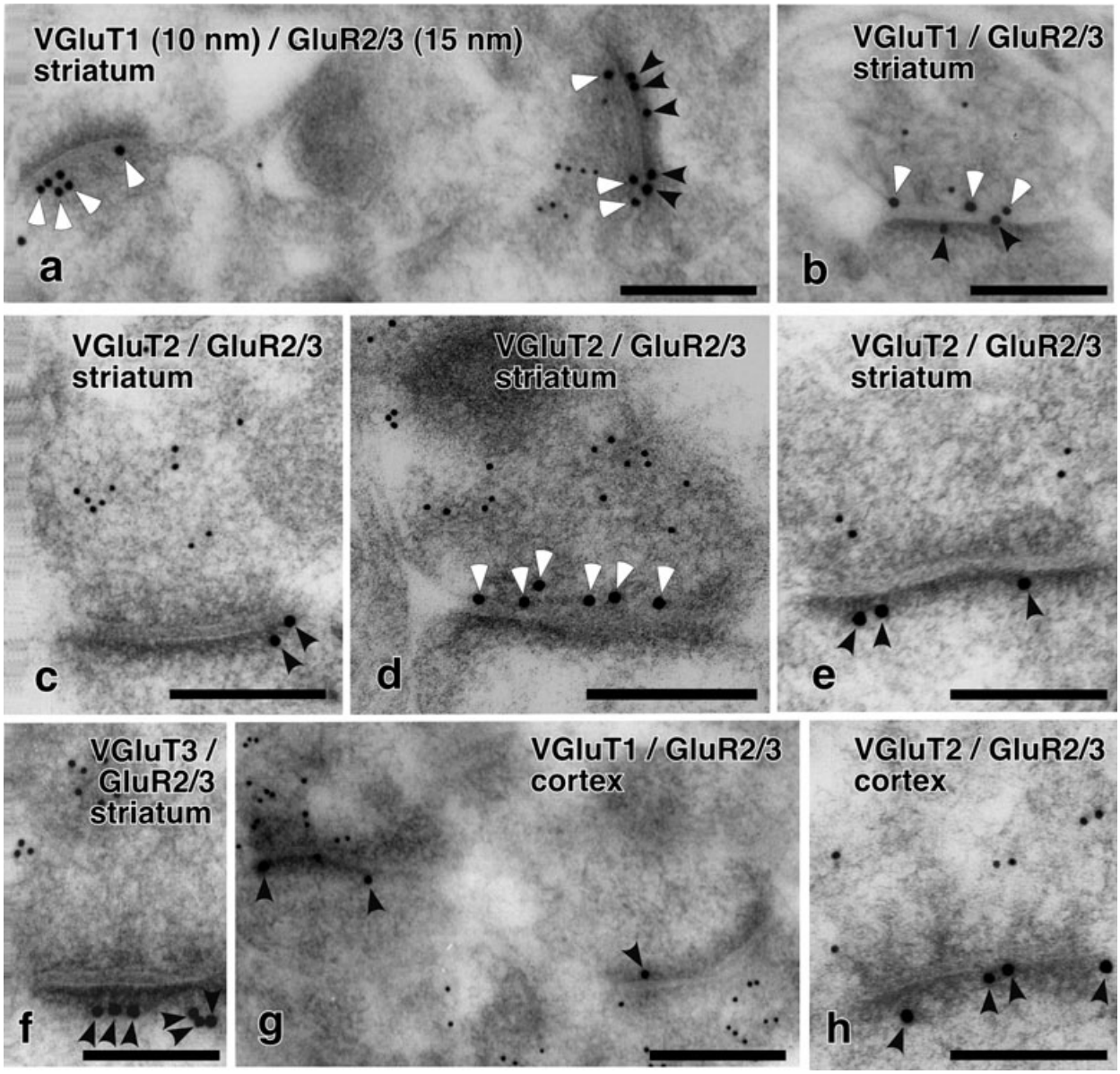

FIG. 2. Post-embedding double immunogold labelling for VGluT and GluR2/3. Small 10-nm and large 15-nm gold particles correspond to immunoreactivities for VGluTs and GluR2/3, respectively. Black and white arrowheads point to GluR2/3-immunoreactive particles at postsynaptic sites and presynaptic sites, respectively. See Results for further details. Scale bars, 200 nm.

anti-GluR1–4 antibodies used in the present study, 15-nm immunogold particles with those anti-GluR2/3 and GluR1 antibodies were found in ≈60 and 20%, respectively, of VGluT-positive asymmetric synapses, suggesting a significant underestimation (at least 40% of synapses) for GluR-immunoreactive synapses in the present method.

In the neostriatum, immunogold particles for GluR1 C-terminal, GluR2[175–430] and GluR2/3 C-terminal were frequently observed at presynaptic sites (Figs 2a, b and d, and 3a–c), as well as at postsynaptic sites (Figs 2a–c and e, and 3a and b) of synapses made between VGluT1- or VGluT2-immunoreactive axon terminals and dendritic profiles with thick postsynaptic specialization. Although much less frequently, immunoreactive particles for GluR4 C-terminals were also found at the presynaptic profiles of VGluT1-immunoreactive synapses (Fig. 3d–g). C-terminal portions of GluR1–4 are known to be located in the intracellular space, whereas GluR2[175–430] is exposed to the extracellular space (for review, see Ozawa *et al*., 1998). In spite of the difference in location of the antigen sites, immunogold particles for GluR2[175–430] were also frequently associated with presynaptic profiles in the neostriatum (Fig. 3h). In contrast, asymmetric synapses with VGluT3-immunopositive axon terminals showed GluR1 and GluR2/3 immunoreactivities almost exclusively at postsynaptic sites (Fig. 2f). In the cerebral cortex, almost all GluR1- and GluR2/3-immunoreactive gold particles were associated with the postsynaptic profiles of VGluT1- and VGluT2-positive asymmetric synapses (Figs 2g and h), indicating that the presynaptic localization of GluR1 and GluR2/3 immunoreactivities was specific to the neostriatal tissue. When the primary antibody for the receptor was omitted or replaced with normal IgG, almost no 15-nm gold particles were found in the neostriatal tissue (data not shown). Further, when the antibody to GluR2/3 C-terminal was preabsorbed with the antigen peptide, gold particles were completely absent in 40 or 45 randomly selected synaptic profiles with VGluT1 or VGluT2 immunoreactivity.

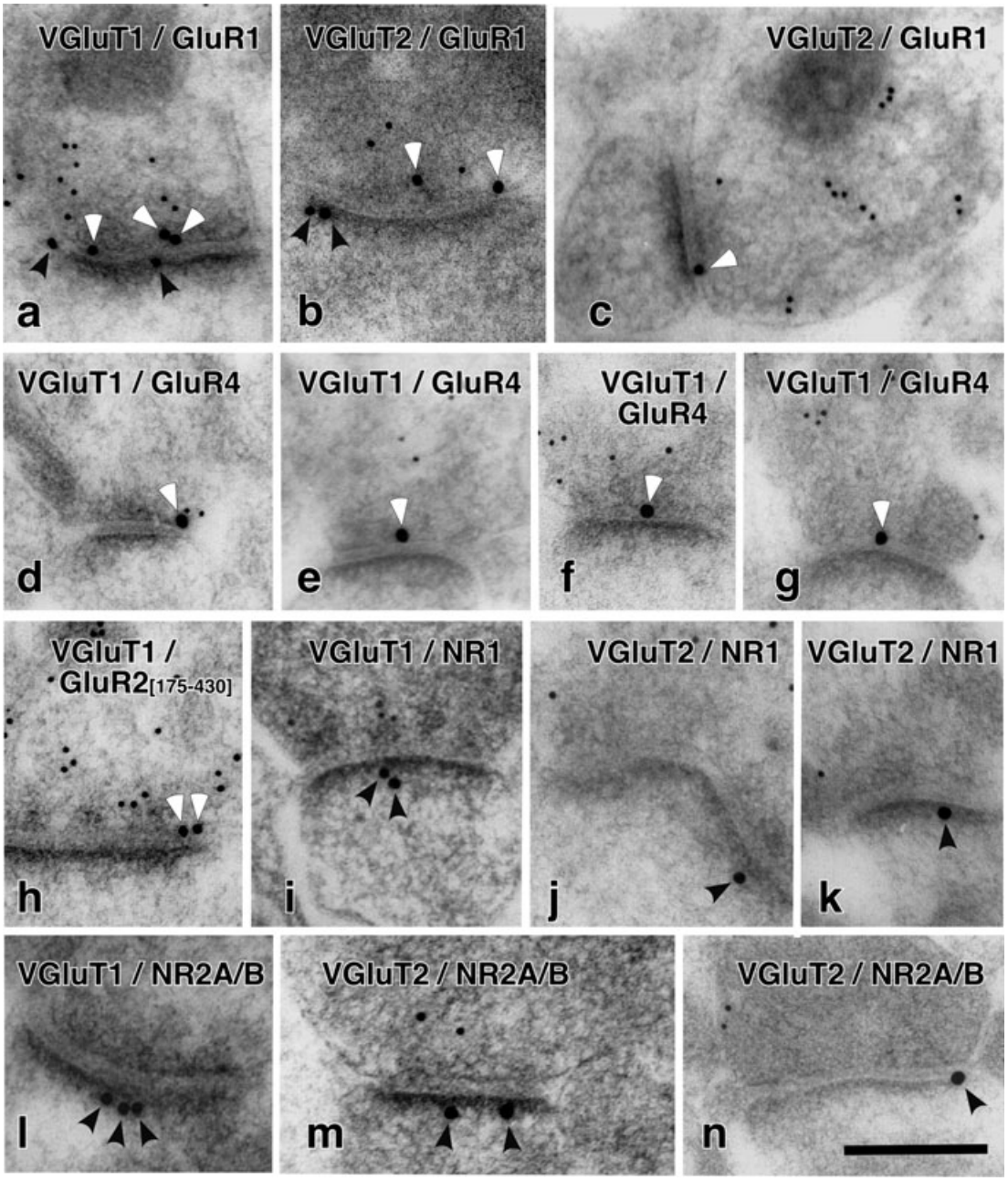

FIG. 3. Post-embedding double immunogold labelling for VGluT and glutamate receptors. Small 10-nm and large 15-nm gold particles correspond to immunoreactivities for VGluTs and glutamate receptors, respectively. Black arrowheads and white arrowheads point to GluR-immunoreactive particles at postsynaptic sites and presynaptic sites, respectively. See Results for further details. Scale bar, 200 nm (a–n).

The distribution of GluR2/3 immunoreactivity is further analysed quantitatively in Fig. 4. The number of immunoreactive gold particles was charted against the relative position in the synaptic structures with the synaptic cleft width normalized to 1. In the neostriatum, at least two peaks were observed for VGluT1- and VGluT2-immunopositive synapses around presynaptic (relative position, −1) and postsynaptic (0) membranes. In contrast, very few particles were observed around the presynaptic membrane in VGluT3-immunopositive synapses of the neostriatum, or in VGluT1- or VGluT2-positive synapses of the cerebral cortex (Fig. 4). GluR2/3-immunoreactive gold particles at presynaptic sites (relative position, −0.5) were $\approx 1/4$ of total immunoreactive particles (27/100) in VGluT1-immunopositive synapses, and 2/5 (40/100) in VGluT2-positive synapses. The difference between VGluT1- and VGluT2-positive synapses was slightly significant by Fisher's one-sided exact probability test ($P = 0.0359$). Although we could not collect 100 immunogold particles because of weak immunolabelling with anti-GluR2[175–430] antibody, 21 of 52 particles detected in VGluT1-positive synapses were observed around presynaptic membrane (relative distance, −0.5), and 23 of 51 particles in VGluT2-positive synapses were found around presynaptic membrane. However, anti-GluR3[245–451] antibody exhibited no immunolabelling in the neostriatum or cerebral cortex by the present postembedding method. Thus, GluR2/3 immunoreactivity was confirmed to contain GluR2 immunoreactivity, but it was not determined whether or not GluR3 immunoreactivity was included in GluR2/3 immunoreactivity.

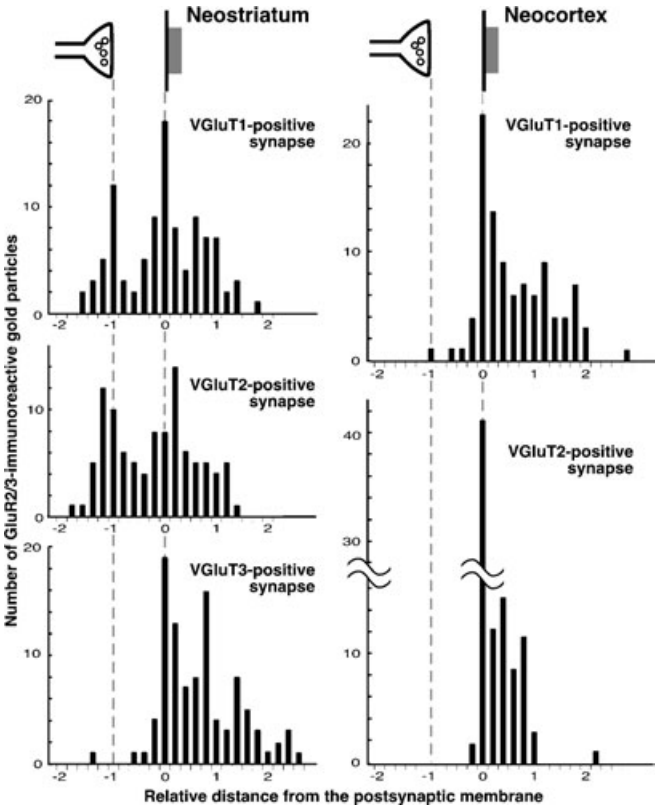

FIG. 4. The distribution of GluR2/3-immunopositive gold particles in the asymmetric synapses where the presynaptic sites were immunopositive for VGluT. Abscissas, relative distance of the centre of gold particles from the outer layer of the presynaptic membrane when the width of synaptic cleft was normalized to 1. Ordinates, the number of particles within a bin of 0.2 relative distance. For each bar chart, 100 gold particles were randomly collected on 31–45 VGluT-positive synaptic profiles in the neostriatum or neocortex.

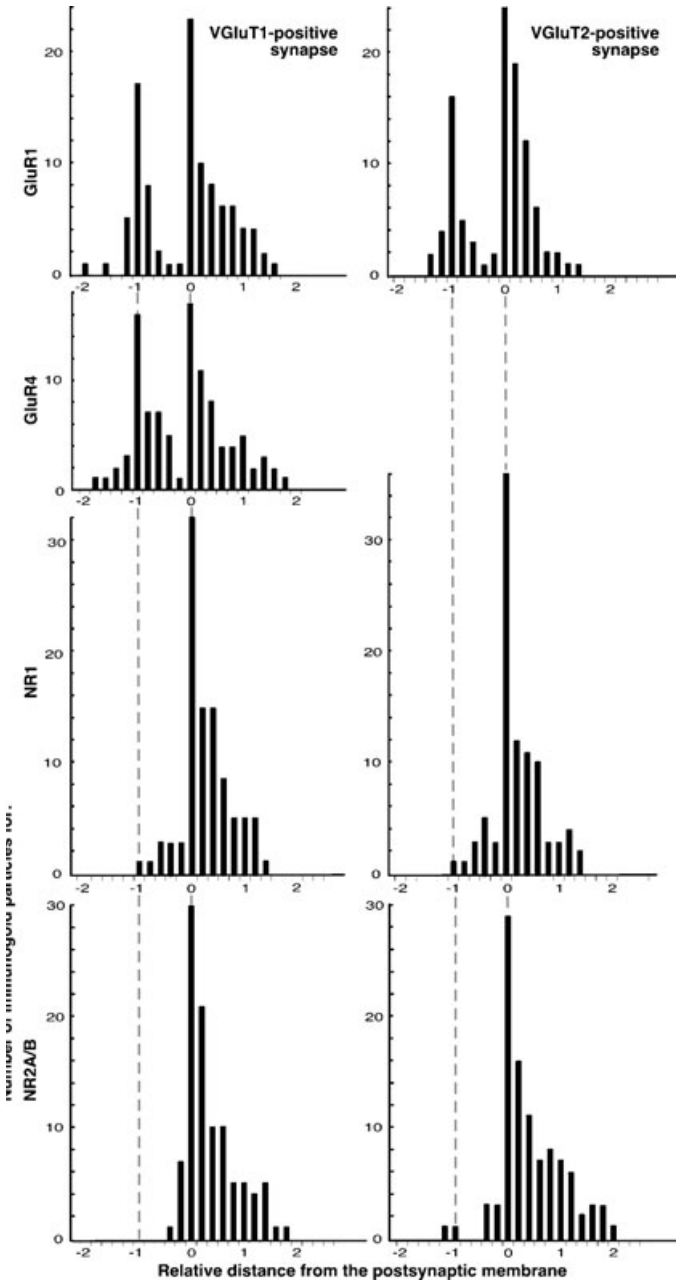

FIG. 5. The distribution of GluR1-, GluR4-, NR1- and NR2A/B-immunopositive gold particles in the asymmetric synapses where the presynaptic sites were immunopositive for VGluT in the neostriatum. Abscissas, relative distance of the centre of gold particles from the outer layer of postsynaptic membrane when the width of the synaptic cleft was normalized to 1. Ordinates, the number of particles within a bin of 0.2 relative distance. For each bar chart, 100 gold particles were randomly collected on 51–86 VGluT-positive synaptic profiles in the neostriatum.

In the upper part of Fig. 5, the distribution of immunoreactive gold particles for GluR1 and GluR4 C-terminals was analysed quantitatively in the neostriatum. Although the frequency of GluR1-immunoreactive particles was less than that of GluR2/3-immunoreactive ones, GluR1-immunoreactive particles were distributed on both presynaptic and postsynaptic profiles of VGluT1- or VGluT2-immunopositive synapses. The proportions of presynaptic particles were 30–37% of total particles. The difference in frequency of presynaptic GluR1-immunoreactive particles between VGluT1- and VGluT2-positive synapses was not statistically significant by one-sided exact probability test ($P = 0.065$). Although GluR1-immunoreactive particles were found in both VGluT1- and VGluT2-positive synapses, GluR4-immunoreactive particles were observed only in VGluT1-positive synapses, where GluR4 immunoreactivity was detected not only in postsynaptic profiles but also in presynaptic profiles as GluR1-3 immunoreactivities. We examined the same number of GluR4-positive synapses in VGluT2/GluR4 double-stained sections as that of GluR4-positive synapses studied in VGluT1/GluR4 double-stained sections ($n = 600$), but observed few VGluT2-immunoreactive particles in GluR4-positive synapses. This suggests that GluR4 is employed only in synapses made by corticostriatal afferents.

In contrast to AMPA receptor subunits, immunogold particles for NMDA receptor subunits, such as NR1 and NR2A/B, were almost always located at the postsynaptic sites in the neostriatum (Fig. 3i–n). This was confirmed by the quantitative analysis in the lower part of Fig. 5; NR1- and NR2A/B-immunoreactive particles only showed a single peak around the postsynaptic membrane of VGluT1- and VGluT2-positive synapses, indicating that almost all functional NMDA receptors were located on postsynaptic sites.

The postsynaptic distribution of NMDA receptor subunits, as well as those of AMPA receptor subunits, were much wider than presynaptic distribution of the receptor subunits and sometimes extended up to 2.5 relative distance (Figs 4 and 5; actually up to 25–50 nm apart from postsynaptic membrane). This intracellular localization of immunogold signals may reflect the internalized

receptor subunits or subunits in preparation (for review, see Bernard *et al*., 1997; Song & Huganir, 2002).

Discussion

The present report is the first line of definitive evidence for the presynaptic localization of AMPA-type glutamate receptors in the neostriatum. Furthermore, the AMPA-type receptor subunits were located on the glutamatergic axon terminals that were derived from both the cerebral cortex and thalamic nuclei, but not on the cholinergic/glutamatergic terminals belonging to striatal interneurons.

Technical consideration and presynaptic localization of glutamate receptors

It is rather well known that ionotropic glutamate receptors in synaptic sites are difficult to label by the pre-embedding immunoelectron-microscopic techniques (Chatha *et al*., 2000). This difficulty might be caused by poor penetration of the antibodies into synaptic structures. Thus, in the present study we employed postembedding with freeze-substitution to label the synaptic glutamate receptors. Actually, in a preliminary study we tried to stain GluR2/3 immunoreactivity by the pre-embedding technique with immunogold and silver enhancement. However, we failed in GluR2/3 labelling, not only at postsynaptic but also at presynaptic sites.

Because the size of IgG is 8 nm and the present immunogold method uses two antibodies serially and immunogold particles with a diameter of 15 nm, the location of gold particles can be up to $(8 \times 2 + 15/2) = 23.5$ nm away from the site of antigen. Taking into consideration that the widths of the lipid bilayer and synaptic cleft are 5 and 10–20 nm, respectively (Peters *et al*., 1991), it is necessary to carefully determine the exact location of glutamate receptors in the synaptic profiles. Thus, we analysed the location of immunogold particles quantitatively (Figs 4 and 5). GluR2/3 immunoreactivity was distributed almost selectively at the postsynaptic sites in VGluT3-positive synapses of the neostriatum and in VGluT1- and VGluT2-positive synapses of the cerebral cortex. Because the latter result is fully consistent with the previous quantitative analysis on the immunogold localization of GluR2/3 in the cerebral cortex (Kharazia & Weinberg, 1999), these results indicate that the postembedding method allowed successful visualization of antigens at postsynaptic sites. Applying the same approach to the neostriatum, we observed GluR2/3-immunoreactive gold particles to be in two peaks around the presynaptic and postsynaptic membranes of synaptic profiles involving VGluT1- and/or VGluT2-positive axon terminals. If the location of GluR2/3-immunoreactive particles was restricted to the postsynaptic membrane, the distribution would have shown only one peak around the postsynaptic membrane. GluR2/3-immunoreactive particles in those synaptic profiles were therefore judged to be distributed not only postsynaptically but also presynaptically. Furthermore, GluR1- and GluR4-immunoreactive particles also exhibited two peaks around the presynaptic and postsynaptic membranes in the neostriatum, supporting the presynaptic localization of AMPA receptor subunits.

The presynaptic localization of AMPA receptor subunits has been reported in some brain regions or at some developmental stages. In the developing striatum, GluR1 immunoreactivity was observed in the presynaptic neurites forming synapses (Martin *et al*., 1998). GluR2- and GluR2/3-immunoreactive gold particles were detected in some presynaptic sites of organotypic hippocampal slices (Fabian-Fine *et al*., 2000). In the retrochiasmatic area and bed nucleus of the stria terminalis, GluR3-immunoreactive axon terminals of oxytocin-containing hypothalamic magnocellular neurons were in synaptic contact with unlabelled dendrites (Ginsberg *et al*., 1995). These findings suggest that AMPA receptors could be located at presynaptic sites in some central synapses. Thus, together with the methodological consideration described above, VGluT1- and VGluT2-positive axon terminals in the neostriatum are considered to truly bear GluR1–3 on their presynaptic membrane.

Sources of AMPA receptors

Layer V pyramidal cells including corticostriatal neurons intensely express mRNA for GluR2, less intensely for GluR1 and GluR3, and weakly for GluR4 (Boulter *et al*., 1990; Keinänen *et al*., 1990; Sommer *et al*., 1990; Pellegrini-Giampietro *et al*., 1991; Gold *et al*., 1997). Though weakly, almost all the thalamic nuclei also display signals for GluR1–4 mRNAs (Boulter *et al*., 1990; Keinänen *et al*., 1990; Sommer *et al*., 1990; Pellegrini-Giampietro *et al*., 1991; Gold *et al*., 1997). In particular, mRNA signals for GluR1 and GluR2 are more intense than those for GluR3 and GluR4 in the intralaminar thalamic nuclei such as the centromedial and parafascicular nuclei (Gold *et al*., 1997), which are well known to send axon fibers to the neostriatum. These findings are consistent with the present results showing that the presynaptic profiles of corticostriatal and thalamostriatal afferents frequently display immunoreactivities for GluR1 and GluR2/3.

Most corticostriatal projection neurons are known to be located in layer V, and layer V pyramidal neurons have some local axon collaterals in the cerebral cortex. Thus, presynaptic AMPA-type glutamate receptors could have been found in VGluT1-positive asymmetric synapses made with those cortical axon collaterals of corticostriatal projection neurons. However, in Fig. 4 almost no GluR2/3-immunoreactive gold particles were found in the presynaptic sites of VGluT1-positive terminals in the cerebral cortex. Because the cerebral cortex contains many axon collaterals of VGluT1-expressing pyramidal cells that are located outside layer V, the frequency of presynaptic AMPA-type receptors might have been too low to be detected in the present study. VGluT2-immunoreactive thalamostriatal afferents originate from the intralaminar nuclei, which also send collateral axon fibers to the cerebral cortex. Although the thalamocortical afferents from the intralaminar nuclei are more diffuse than those from specific relay nuclei such as the ventrobasal nucleus, they are distributed in most cortical layers through layer I to layer VI. Thus, if the cortical axon collaterals of thalamostriatal projection neurons had presynaptic AMPA-type receptors, we would expect some GluR2/3-immunoreactivity in the presynaptic sites of VGluT2-positive terminals. However, in the present quantitative analysis, VGluT2-positive axon terminals in the cerebral cortex showed almost no GluR2/3 immunoreactivity (Fig. 4). It may be that AMPA-type receptors are located in the corticostriatal and thalamostriatal afferents but not in their cortical collaterals.

GluR4-immunoreactive gold particles were only occasionally observed in the neostriatum where they were restricted to the synaptic profiles showing VGluT1 immunoreactivity. As described above, not only layer V pyramidal cells but also intralaminar thalamic neurons were positive for GluR4 mRNA, although the mRNA signals were weak. Thus, presynaptic GluR4 immunoreactivity could be expected to be observed in both VGluT2-positive and VGluT1-positive axon terminals. We examined VGluT2/GluR4-double stained sections as extensively as VGluT1/GluR4-double stained sections, but did not find any GluR4 immunoreactivity in VGluT2-positive synapses.

GluR4 mRNA is expressed only by some interneurons in the neostriatum (Bernard *et al*., 1997). It is likely that these interneurons receive cortical but not thalamic afferents and thus that postsynaptic GluR4 immunoreactivity is restricted to corticostriatal synapses. However, it remains to be resolved why presynaptic GluR4 immunoreactivity was confined to VGluT1-positive corticostriatal synapses.

It has been reported that neostriatal cholinergic neurons express VGluT3 mRNA, and most cholinergic axon terminals in the neostriatum are positive for VGluT3 immunoreactivity (Gras *et al*., 2002). These findings are supported by the present result that almost all VGluT3-immunoreactive axon terminals showed immunoreactivity for vesicular acetylcholine transporter (Fig. 1h). In addition, the postsynaptic membranes of VGluT3-positive synapses were almost always enriched in postsynaptic density and immunopositive for GluR2/3 (Figs 2f and 4) and GluR1 (F. Fujiyama, unpublished observation). This indicates that neostriatal cholinergic interneurons are highly likely to produce EPSPs in their target neurons if glutamate is coreleased with acetylcholine from their axon terminals.

Functions of presynaptic AMPA receptors

Recently, Patel *et al*. (2001), using the *in vivo* microdialysis method, reported that application of AMPA increased glutamate release from the rat neostriatum in a dose-dependent manner, and that the increase was blocked by competitive AMPA antagonists. More recently, Dohovics *et al*. (2003) observed that AMPA-evoked glutamate release from striatal glutamatergic terminals was potentiated by β-adrenergic receptor-mediated cAMP accumulation. These observations are supported by the present results indicating the presynaptic localization of AMPA receptor subunits in corticostriatal and thalamostriatal afferents. This AMPA-receptor-mediated positive feedback mechanism may produce nonlinear effects on the postsynaptic striatal neurons and play an important role in a range of physiological processes including 'up'–'down' state transition and synaptic plasticity.

Medium-sized spiny striatal neurons are known to have two states *in vivo*, 'up' and 'down' states (for review, see Kerr & Plenz, 2002). The neurons alternatively keep their membrane potential at a level far below the threshold in the 'down' state, or at a subthreshold level in the 'up' state, which is produced by massive corticostriatal and/or thalamostriatal afferents and regarded as a ready-to-fire condition. The positive feedback mechanism of corticostriatal and thalamostriatal inputs seems useful in 'down'-to-'up' state transition or switching, because those afferents can work in an all-or-none manner by the nonlinearity of the positive feedback mechanism. On the other hand, presynaptic localization of metabotropic glutamate receptors (mGluR), group II and group III mGluRs, is well known in the corticostriatal axon terminals, and activation of group III mGluRs is considered to suppress or inhibit the presynaptic axon terminals (for review, see Rouse *et al*., 2000). Group III mGluRs on the presynaptic terminals are conceivably activated during the 'up' state by glutamate released from the terminals; thus, the activation of mGluRs may result in a shut-down of the positive feedback mechanism involving presynaptic AMPA receptor and the cessation of the 'up' state. The corticostriatal and thalamostriatal afferents might hence control 'up'–'down' state transition of striatal neurons through the interaction of presynaptic AMPA receptors and mGluRs. In conclusion, corticotsriatal and thalamostriatal afferents are likely to use a positive feedback mechanism that relies on presynaptic AMPA autoreceptors.

Acknowledgements

The work was funded by Grants-in-Aid from the Ministry of Education, Science, Sports, and Culture of Japan: Grant number 15029224, Grant Number 16200025 and Grant Number 16500217. We would like to thank Dr E. L. White, Dr A. Keller, Dr P. Somogyi, Dr C. B. Saper, Dr K. Rockland and Dr T. Hökfelt for their helpful comments on the results of the manuscript.

Abbreviations

BDA, biotinylated dextran amine; mGluR, metabotropic glutamate receptor; PB, 0.1 M phosphate–NaOH buffer, pH 7.4; PBS, phosphate-buffered saline; TBS, 50 mM Tris–HCl-buffered 0.9% saline, pH 7.4; TBS-T, TBS containing 0.01% Triton X-100; TBS-TA, TBS-T containing 2% human serum albumin; VGluT, vesicular glutamate transporter.

References

Alexi, T., Borlongan, C.V., Faull, R.L., Williams, C.E., Clark, R.G., Gluckman, P.D. & Hughes, P.E. (2000) Neuroprotective strategies for basal ganglia degeneration: Parkinson's and Huntington's disease. *Prog. Neurobiol.*, **60**, 409–470.

Bai, L., Xu, H., Collins, J.F. & Ghishan, F.K. (2001) Molecular and functional analysis of a novel neuronal vesicular glutamate transporter. *J. Biol. Chem.*, **276**, 36764–36769.

Bernard, V., Somogyi, P. & Bolam, J.P. (1997) Cellular, subcellular, and subsynaptic distribution of AMPA-type glutamate receptor subunits in the neostriatum of the rat. *J. Neurosci.*, **17**, 819–833.

Boulter, J., Hollmann, M., O'Shea-Greenfield, A., Hartley, M., Deneris, E., Maron, C. & Heinemann, S. (1990) Molecular cloning and functional expression of glutamate receptor subunit genes. *Science*, **249**, 1033–1037.

Calabresi, P., Centonze, D., Gubellini, P., Marfia, G.A., Pisani, A., Sancesario, G. & Bernardi, G. (2000) Synaptic transmission in the striatum: from plasticity to neurodegeneration. *Prog. Neurobiol.*, **61**, 231–265.

Chatha, B.T., Bernard, V., Streit, P. & Bolam, J.P. (2000) Synaptic localization of ionotropic glutamate receptors in the rat substantia nigra. *Neuroscience*, **101**, 1037–1051.

Dohovics, R., Janaky, R., Varga, V., Hermann, A., Saransaari, P. & Oja, S.S. (2003) Regulation of glutamatergic neurotransmission in the striatum by presynaptic adenylyl cyclase-dependent processes. *Neurochem. Int.*, **42**, 1–7.

Fabian-Fine, R., Volknandt, W., Fine, A. & Stewart, M.G. (2000) Age-dependent pre- and postsynaptic distribution of AMPA receptors at synapses in CA3 stratum radiatum of hippocampal slice cultures compared with intact brain. *Eur. J. Neurosci.*, **12**, 3687–3700.

Fremeau, R.T. Jr, Troyer, M.D., Pahner, I., Nygaard, G.O., Tran, C.H., Reimer, R.J., Bellocchio, E.E., Fortin, D., Storm-Mathisen, J. & Edwards, R.H. (2001) The expression of vesicular glutamate transporters defines two classes of excitatory synapse. *Neuron*, **31**, 247–260.

Fujiyama, F., Furuta, T. & Kaneko, T. (2001) Immunocytochemical localization of candidates for vesicular glutamate transporters in the rat cerebral cortex. *J. Comp. Neurol.*, **435**, 379–387.

Ginsberg, S.D., Martin, L.J. & Rothstein, J.D. (1995) Regional differentiation down-regulates subtypes of glutamate transporter proteins. *J. Neurochem.*, **65**, 2800–2803.

Gold, S.J., Ambros-Ingerson, J., Horowitz, J.R., Lynch, G. & Gall, C.M. (1997) Stoichiometries of AMPA receptor subunit mRNAs in rat brain fall into discrete categories. *J. Comp. Neurol.*, **385**, 491–502.

Gras, C., Herzog, E., Bellenchi, G.C., Bernard, V., Ravassard, P., Pohl, M., Gasnier, B., Giros, B. & El Mestikawy, S. (2002) A third vesicular glutamate transporter expressed by cholinergic and serotoninergic neurons. *J. Neurosci.*, **22**, 5442–5451.

Herzog, E., Bellenchi, G.C., Gras, C., Bernard, V., Ravassard, P., Bedet, C., Gasnier, B., Giros, B. & El Mestikawy, S. (2001) The existence of a second vesicular glutamate transporter specifies subpopulations of glutamatergic neurons. *J. Neurosci.*, **21**, RC181.

Hioki, H., Fujiyama, F., Furuta, T. & Kaneko, T. (2004) Immunocytochemical localization of vesicular glutamate transporter 3 in rat cerebral cortex. *Neurosci. Res.*, **46**, S176.

Hioki, H., Fujiyama, F., Taki, K., Tomioka, R., Furuta, T., Tamamaki, N. & Kaneko, T. (2003) Differential distribution of vesicular glutamate transporters in the rat cerebellar cortex. *Neuroscience*, **117**, 1–6.

Hisano, S., Hoshi, K., Ikeda, Y., Maruyama, D., Kanemoto, M., Ichijo, H., Kojima, I., Takeda, J. & Nogami, H. (2000) Regional expression of a gene

encoding a neuron-specific Na (+)-dependent inorganic phosphate cotransporter (DNPI) in the rat forebrain. *Brain Res. Mol. Brain Res.*, **83**, 34–43.

Kaneko, T., Fujiyama, F. & Hioki, H. (2002) Immunohistochemical localization of candidates for vesicular glutamate transporters in the rat brain. *J. Comp. Neurol.*, **444**, 39–62.

Keinänen, K., Wisden, W., Sommer, B., Werner, P., Herb, A., Verdoorn, T.A., Sakmann, B. & Seeburg, P.H. (1990) A family of AMPA-selective glutamate receptors. *Science*, **249**, 556–560.

Kerr, J.N.D. & Plenz, D. (2002) Dendritic calcium encodes striatal neuron output during up-states. *J. Neurosci.*, **22**, 11499–11512.

Kharazia, V.N. & Weinberg, R.J. (1999) Immunogold localization of AMPA and NMDA receptors in somatic sensory cortex of albino rat. *J. Comp. Neurol.*, **412**, 292–302.

Martin, L.J., Furuta, A. & Blackstone, C.D. (1998) AMPA receptor protein in developing rat brain: glutamate receptor-1 expression and localization change at regional, cellular, and subcellular levels with maturation. *Neuroscience*, **83**, 917–928.

Ni, B., Rosteck, P.R. Jr, Nadi, N.S. & Paul, S.M. (1994) Cloning and expression of a cDNA encoding a brain-specific Na (+)-dependent inorganic phosphate cotransporter. *Proc. Natl Acad. Sci. USA*, **91**, 5607–5611.

Ni, B., Wu, X., Yan, G.M., Wang, J. & Paul, S.M. (1995) Regional expression and cellular localization of the Na (+)-dependent inorganic phosphate cotransporter of rat brain. *J. Neurosci.*, **15**, 5789–5799.

Nusser, Z., Sieghart, W. & Somogyi, P. (1998) Segregation of different $GABA_A$ receptors to synaptic and extrasynaptic membranes of cerebellar granule cells. *J. Neurosci.*, **18**, 1693–1703.

Ozawa, S., Kamiya, H. & Tsuzuki, K. (1998) Glutamate receptors in the mammalian central nervous system. *Prog. Neurobiol.*, **54**, 581–618.

Patel, D.R., Young, A.M. & Croucher, M.J. (2001) Presynaptic alpha-amino-3-hydroxy-5-methyl-4-isoxazole propionate receptor-mediated stimulation of glutamate and GABA release in the rat striatum in vivo: a dual-label microdialysis study. *Neuroscience*, **102**, 101–111.

Pellegrini-Giampietro, D.E., Bennett, M.V. & Zukin, R.S. (1991) Differential expression of three glutamate receptor genes in developing rat brain: an in situ hybridization study. *Proc. Natl Acad. Sci. USA*, **88**, 4157–4161.

Peters, A., Palay, S.L. & Webster, H. (1991) *The Fine Structure of the Nervous System*, 3rd edn. Oxford University Press, New York.

Rouse, S.T., Marino, M.J., Bradley, S.R., Awad, H., Wittmann, M. & Conn, P.J. (2000) Distribution and roles of metabotropic glutamate receptors in the basal ganglia motor circuit: implications for treatment of Parkinson's disease and related disorders. *Pharmacol. Ther.*, **88**, 427–435.

Smith, A.D. & Bolam, J.P. (1990) The neural network of the basal ganglia as revealed by the study of synaptic connections of identified neurones. *Trends Neurosci.*, **13**, 259–265.

Sommer, B., Keinänen, K., Verdoorn, T.A., Wisden, W., Burnashev, N., Herb, A., Kohler, M., Takagi, T., Sakmann, B. & Seeburg, P.H. (1990) Flip and flop: a cell-specific functional switch in glutamate-operated channels of the CNS. *Science*, **249**, 1580–1585.

Song, I. & Huganir, R.L. (2002) Regulation of AMPA receptors during synaptic plasticity. *Trends Neurosci.*, **25**, 578–588.